

## A Suggested Final Configuration for the Very Large Array

J. M. WROBEL<sup>1</sup> AND R. C. WALKER<sup>1</sup>

<sup>1</sup>*National Radio Astronomy Observatory, P.O. Box O, Socorro, NM 87801, USA*

(Received 2022 May 13 as ngVLA Memo # 97 for consideration by the VLA/VLBA to ngVLA Transition Advisory Group)

### ABSTRACT

If the construction of the ngVLA begins in 2026, its sensitivity is expected to match that of the VLA by late 2029. At that juncture it is anticipated that open-skies observing will cease on the VLA and commence on the ngVLA. We suggest that during 2026-2029 the VLA be held in a customized final configuration encompassing portions of its standard A, B, C and D configurations. Such a final VLA configuration would (1) help minimize the cost of VLA operations and maximize the pace of ngVLA construction and commissioning; (2) help VLA users pivot to the high-resolution, high-frequency research topics that are projected to headline the ngVLA science program; and (3) help mitigate the effects of source confusion during responses to transients in the era of the Rubin Observatory and LIGO A+.

*Keywords:* Interferometry (808)

### 1. CONTEXT AND MOTIVATION

The next-generation VLA (ngVLA) is envisaged to be an interferometric array operating at frequencies between 1.2 and 116 GHz, with ten times the sensitivity and angular resolution of the VLA and ALMA (Murphy et al. 2018; Selina et al. 2018; McKinnon et al. 2019). If the construction of the ngVLA begins in 2026, its sensitivity is expected to approximately match that of the VLA by late 2029.<sup>1</sup> At that juncture it is expected that PI-driven, open-skies observing will cease on the VLA and commence on the ngVLA as Early Science (Ford et al. 2019). The NRAO has begun working with the community to identify and evaluate possible options for such a transition.<sup>2</sup> In the interim we are guided by some draft concepts mentioned by Chandler et al. (2019), notably the possibility that the VLA continue to operate at a reduced level during 2026-2029.

Here, we explore a hypothetical reduction in one capability of the VLA, namely its reconfigurability. Specifically, we suggest that the VLA be held in a customized final configuration encompassing portions of its standard

A, B, C and D configurations. Such a final VLA configuration would (1) help minimize the cost of VLA operations and maximize the pace of ngVLA construction and commissioning, by freeing staff from VLA reconfiguration activities; (2) help VLA users pivot to the high-resolution, high-frequency research topics that are projected to headline the ngVLA science program (Murphy et al. 2018; Wrobel & Murphy 2020; Wrobel et al. 2020); and (3) help mitigate the effects of host-galaxy and cosmological confusion during responses to transients in the era of the Rubin Observatory and LIGO A+ (Ivezic et al. 2019; Reitze et al. 2019).

### 2. APPROACH AND RESULTS

For each of its standard A, B, C and D configurations, the VLA offers a power-law spacing of the nine antennas placed along each of its three equiangular arms (Thompson et al. 1980; Napier et al. 1983). The distance  $d_n$  from the center of the array of the  $n^{\text{th}}$  antenna per arm, counting outward from the center, is proportional to  $n^{1.716}$ . The different standard configurations have different proportionality constants. The values chosen for those constants offer two advantages. First, it means that some antenna pads can be shared among the configurations, so only 24 pads per arm are needed to accommodate all standard configurations. Those pad locations are shown in Figure 1. Below, we will make use of each arm's 24 standard pad identifiers  $p$  that span 1 to 72 with

Corresponding author: J. M. Wrobel  
jwrobel@nrao.edu

<sup>1</sup> <https://ngvla.nrao.edu/>

<sup>2</sup> <https://science.nrao.edu/enews/15.5/>

gaps (see Table 1 in Thompson et al. 1980). Second, the scaling between the standard configurations resembles that between three of the VLA’s original observing bands, facilitating imaging at matched angular resolutions among those bands. With the advent of complete frequency coverage between 1 and 50 GHz on the VLA (Perley et al. 2011) and robust data-weighting schemes (Briggs 1995), this second advantage has become less significant.

We suggest that during 2026-2029 the VLA be held in a customized final configuration encompassing portions of all its standard configurations. We opt to avoid populating the two innermost pads per arm,  $p = 1$  and  $p = 2$ , as such short spacing information can be obtained with single dish facilities. We also opt to avoid populating the outermost pad per arm,  $p = 72$ , as this will help reduce the operational burden. This leaves us with a set of 21 pad locations per arm that we wish to populate with nine antennas per arm. To do so, we take two steps.

First, we seek a power-law spacing of the nine antennas per arm, spread between the innermost antenna’s  $d_1 = 89.9$  m on pad  $p = 3$  and the outermost antenna’s  $d_9 = 17160.8$  m on pad  $p = 64$ . These extremes define a power-law exponent  $\log_{10}(d_9/d_1)/\log_{10}(9) = 2.390$  and lead to the set of nine desired distances  $d_n^{desired}$  given in Table 1.

Second, for simplicity we invoke the VLA’s power-law model for its pad locations per arm. We then search among pads  $p = 4, \dots, 56$  per arm to find the seven pads that come closest to achieving the desired distances  $d_n^{desired}$  for seven additional antennas. The seven closest-pad identifiers plus the two end-defining pads are given in Table 1, along with their closest-pad distances  $d_n$ .

The closest-pad identifiers in Table 1 define our suggestion for the VLA’s final configuration. Armed with those identifiers, we use **SCHED** to access their catalogued

locations and generate  $(u, v)$  coverage plots for short (0.2 hour) and long (8.0 hour) tracks, subject to an antenna elevation limit of 15 degrees. The  $(u, v)$  coverage plots are shown on A-configuration scales in Figures 2 and 3, on B-configuration scales in Figures 4 and 5, on C-configuration scales in Figures 6 and 7, and on D-configuration scales in Figures 8 and 9. These figures indicate reasonable  $(u, v)$  coverage on the standard scales long familiar to VLA users.

### 3. SUMMARY AND NEXT STEPS

We explored a hypothetical reduction in one capability of the VLA, namely its reconfigurability, during the years of a VLA-to-ngVLA transition. We identified a power-law configuration for the VLA that involves portions of its standard A, B, C and D configurations. We suggested that the VLA be held in this final, customized configuration during the transition years, and mentioned some operational and scientific advantages of doing so.

A specific next step is to use simulations to study the performance parameters and image fidelity of our suggested final configuration for the VLA. We look forward to learning the community’s reaction to our suggestion. We also look forward to learning about the alternate ideas that will emerge as the NRAO engages with community stakeholders to identify and evaluate possible options for the VLA/VLBA-to-ngVLA transition.

### ACKNOWLEDGMENTS

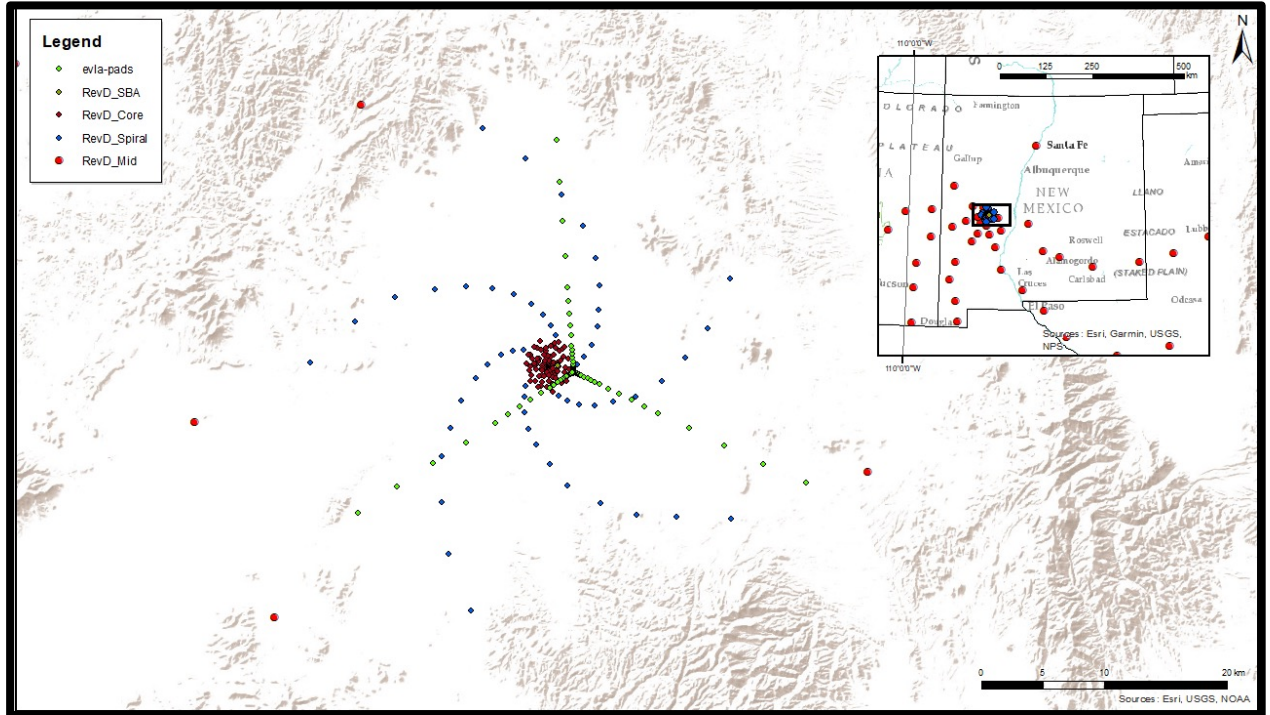
We thank Joe Carilli for generating Figure 1. The NRAO is a facility of the National Science Foundation (NSF), operated under cooperative agreement by AUI. The ngVLA is a design and development project of the NSF operated under cooperative agreement by AUI.

### REFERENCES

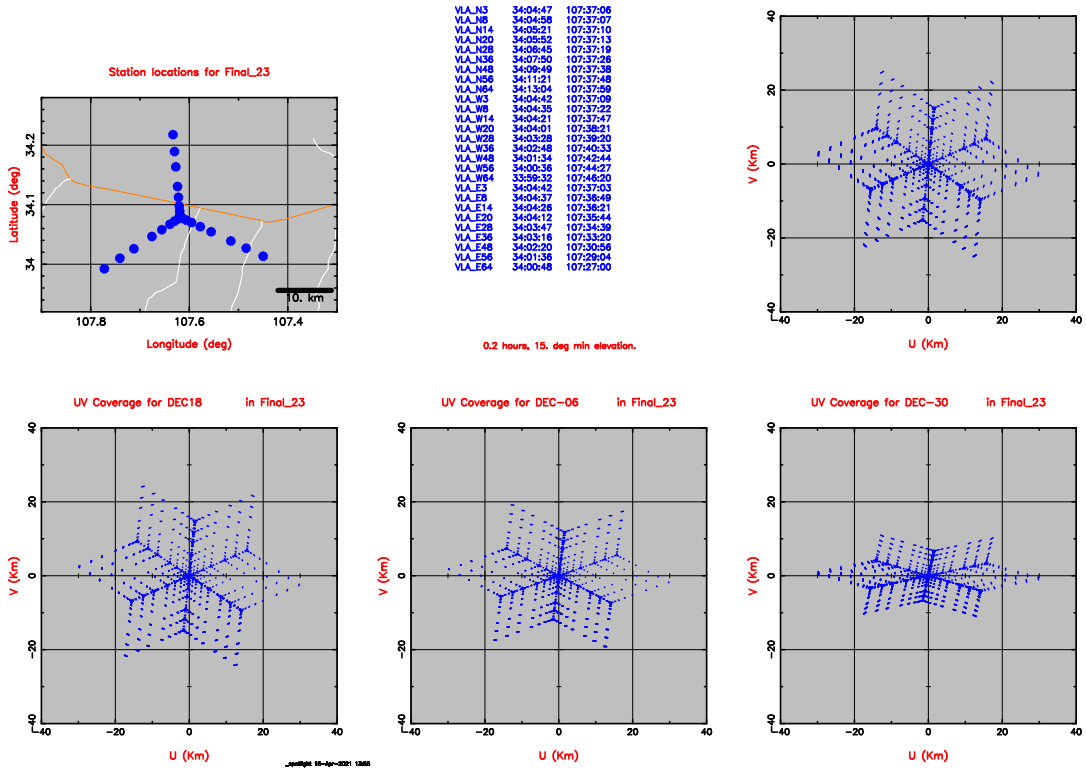
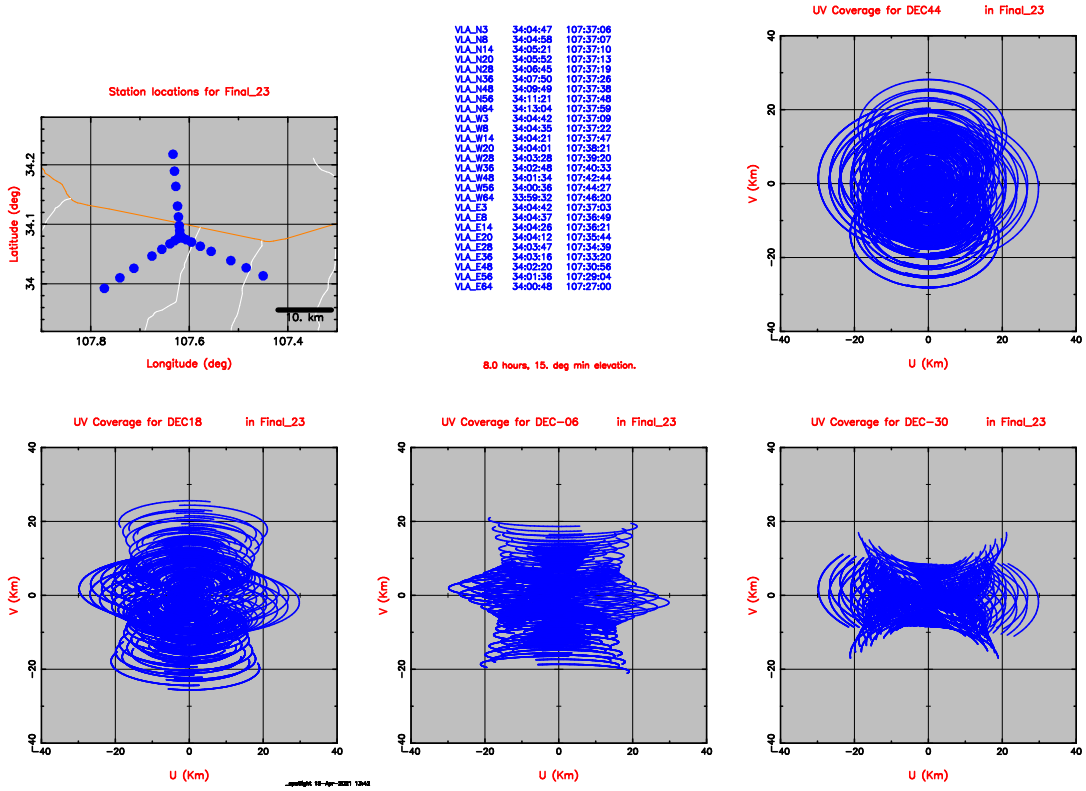
- Briggs, D. S. 1995, Ph. D. thesis, New Mexico Tech
- Carilli, C. et al. 2022, NRAO Doc. #: 020.23.00.00.00-0002-DSN, Revision B
- Chandler, C. et al. 2019, NRAO Doc. #: 020.10.05.00.00-0003-PLA, Revision 0.4
- Ford, E. et al. 2019, NRAO Doc. #: 020.10.05.00.00-0002-PLA, Revision C
- Ivezic, Z., et al. 2019, AJ, 873, 111
- McKinnon, M. M., et al. 2019, BAAS, Vol. 51, Issue 7, id. 81
- Murphy, E. J., et al. 2018, in ASP Conf. Ser. 517, 3
- Napier, P. J., Thompson, A. R., & Ekers, R. D. 1983, Proc. IEEE, 71, 1295
- Perley, R. A., Chandler, C. C., Butler, B. J., & Wrobel, J. M. 2011, ApJL, 739, L1
- Reitze, D., et al. 2019, BAAS, Vol. 51, Issue 7, id. 141
- Selina, R. J., et al. 2018, in ASP Conf. Ser. 517, 15
- Thompson, A. R., Clark, B. G., Wade, C. M., & Napier, P. J. 1980, ApJS, 44, 151
- Wrobel, J. M., & Murphy, E. J. 2020, NRAO Doc. #: 020.10.15.05.10-0001-REP, Revision B
- Wrobel, J. M., Mason, B. S., & Murphy, E. J. 2020, NRAO Doc. #: 020.10.15.05.10-0002-REP, Revision A

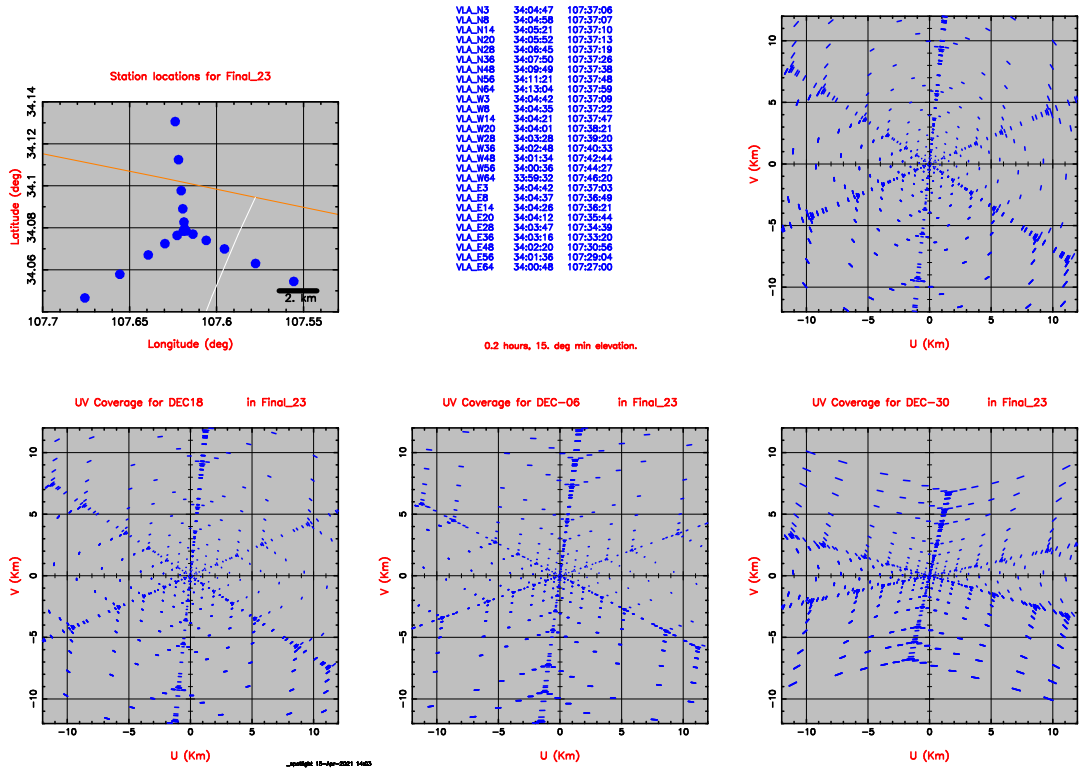
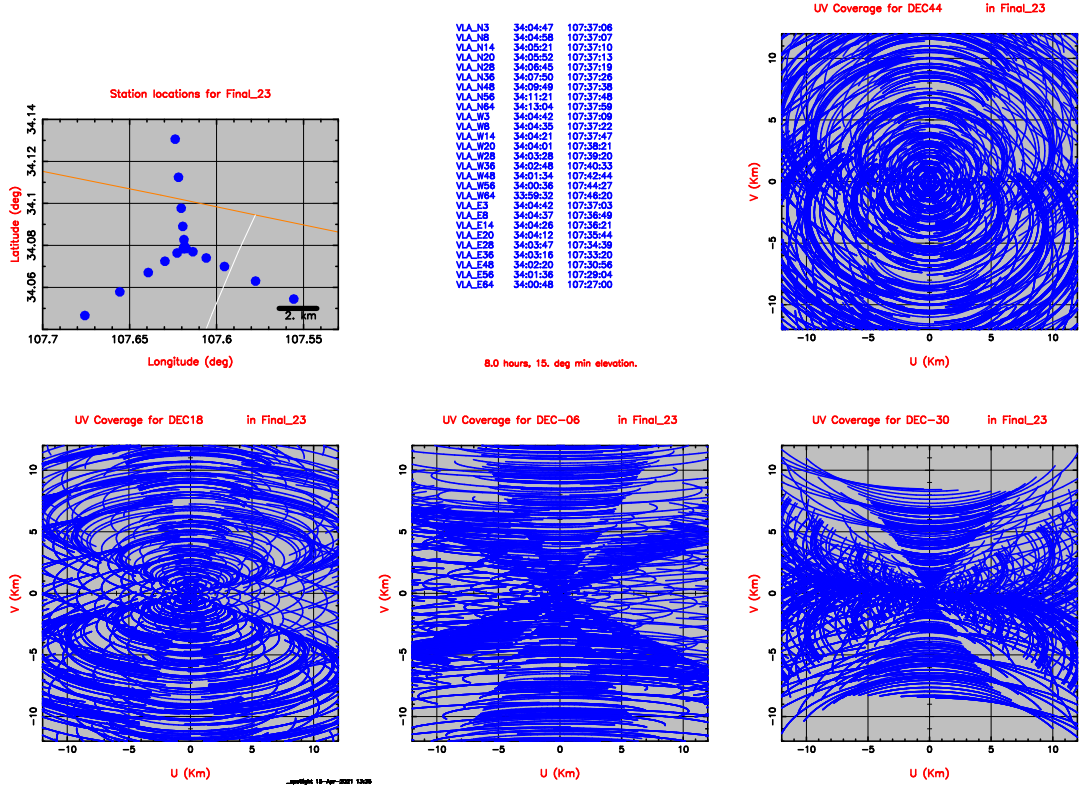
**Table 1.** A Suggested Final Configuration for the VLA

(1)	(2)	(3)	(4)	(5)	(6)	(7)	(8)	(9)	(10)
Antenna index, $n$	1	2	3	4	5	6	7	8	9
Desired distance, $d_n^{desired}$ (m)	89.9	471.3	1242.1	2470.4	4211.1	6511.1	9411.7	12950.2	17160.8
Closest pad identifier, $p$	3	8	14	20	28	36	48	56	64
Closest pad distance, $d_n$ (m)	89.9	484.0	1264.4	2331.8	4153.9	6393.6	10474.7	13646.6	17160.8

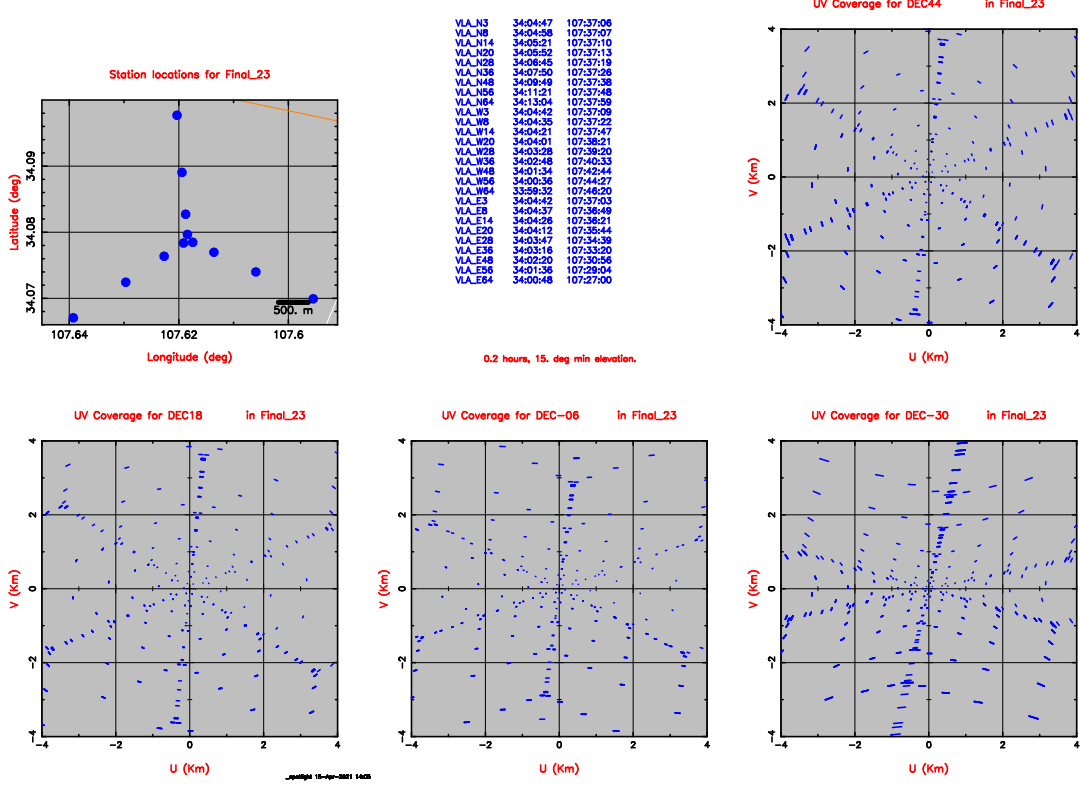
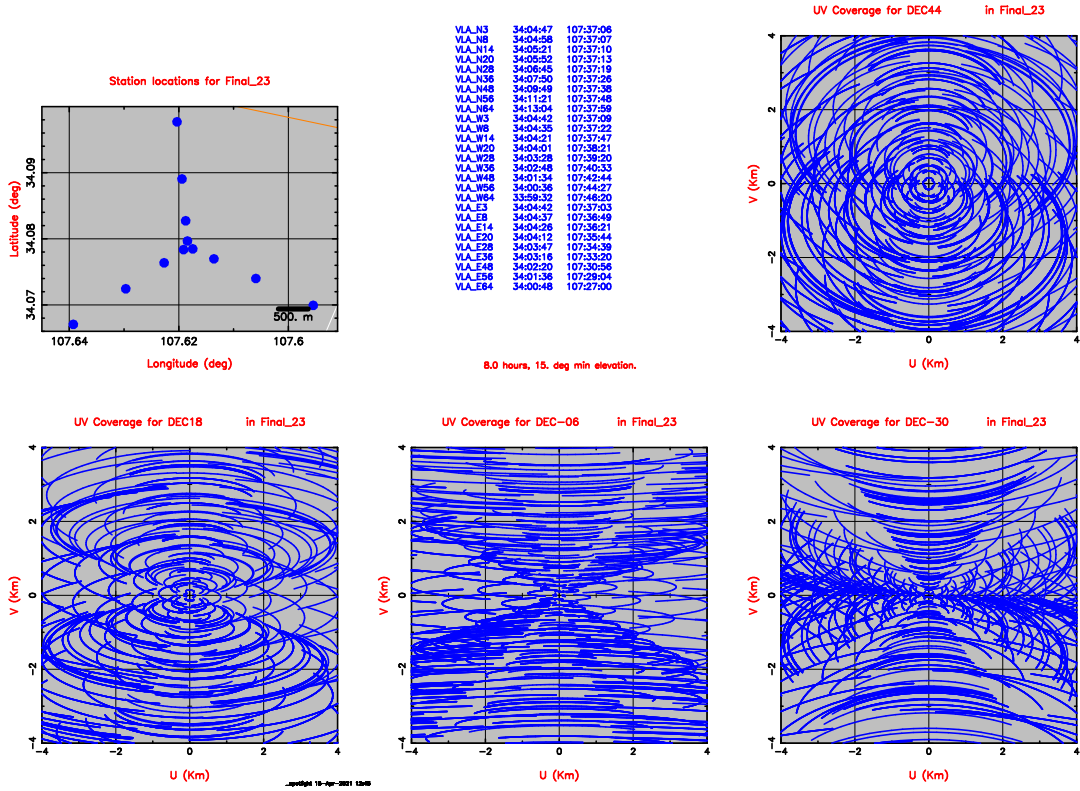


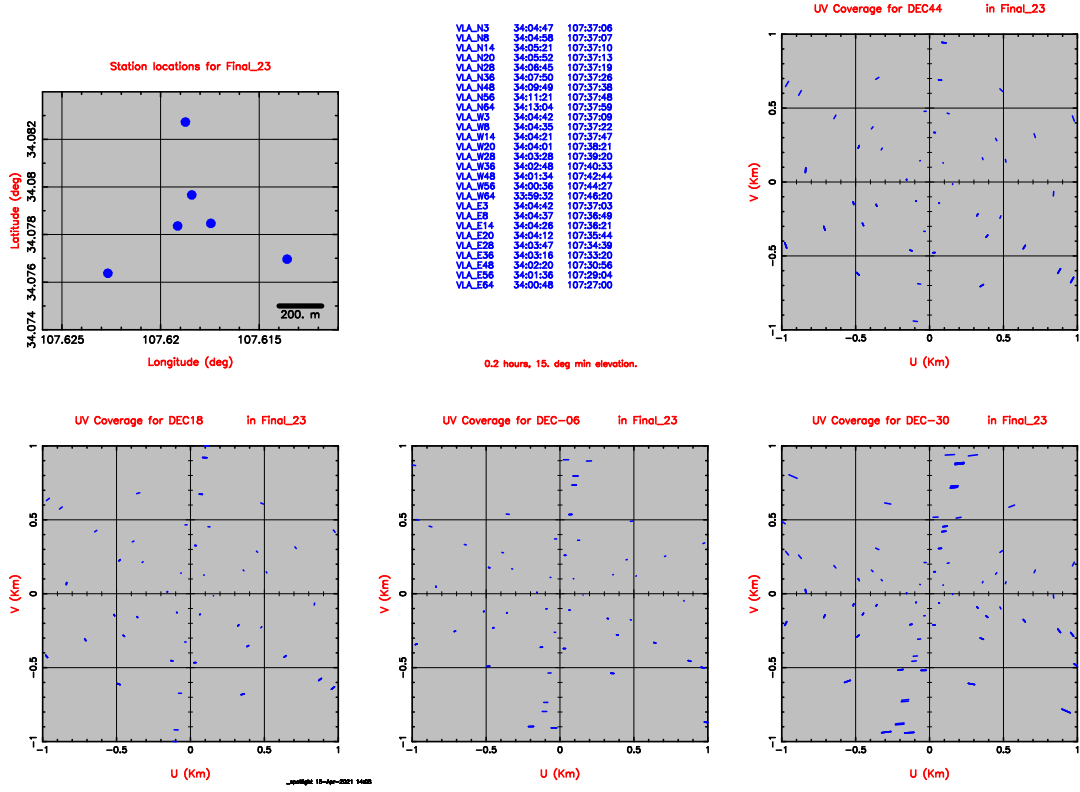
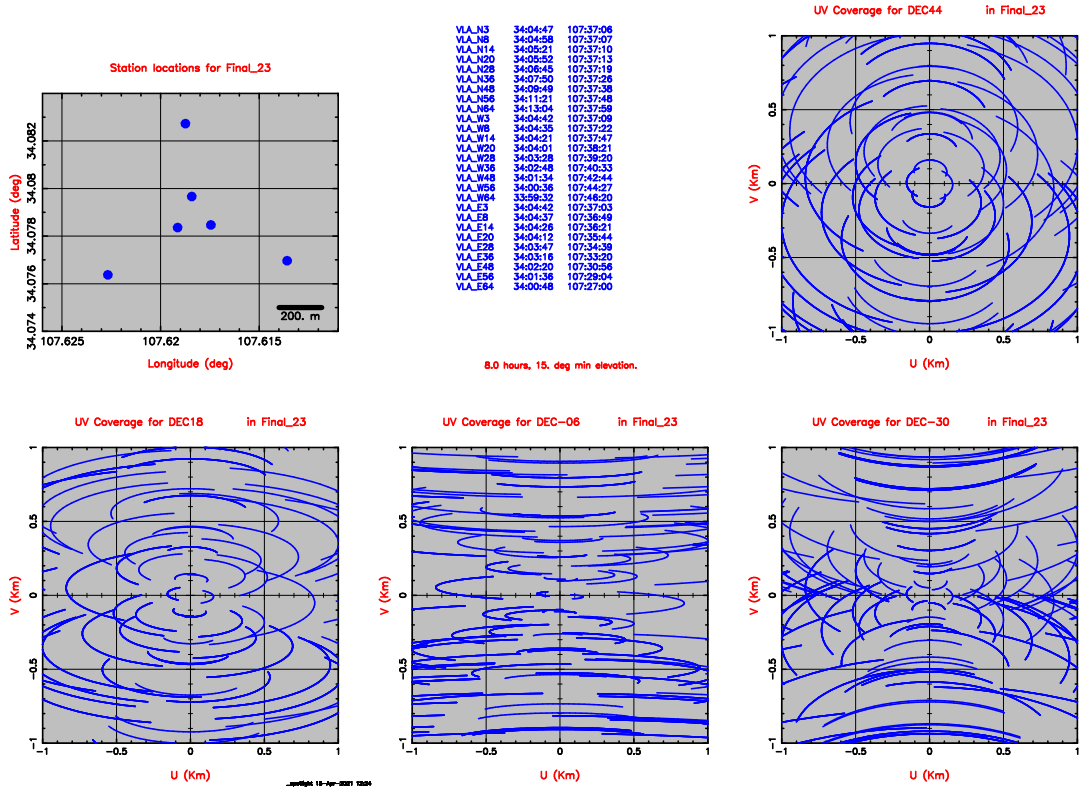
**Figure 1.** Map of the Plains of San Agustin, New Mexico, USA. Green symbols mark the 24 standard pad locations on each arm of the VLA. Other symbols mark potential Rev D locations of ngVLA antennas. Terrain features are also indicated. Adapted from Carilli et al. (2022).

Figure 2.  $(u, v)$  coverage over  $\pm 40$  km. Short track.Figure 3.  $(u, v)$  coverage over  $\pm 40$  km. Long track.

Figure 4.  $(u, v)$  coverage over  $\pm 12$  km. Short track.Figure 5.  $(u, v)$  coverage over  $\pm 12$  km. Long track.



Figure 6.  $(u, v)$  coverage over  $\pm 4$  km. Short track.Figure 7.  $(u, v)$  coverage over  $\pm 4$  km. Long track.

Figure 8.  $(u, v)$  coverage over  $\pm 1$  km. Short track.Figure 9.  $(u, v)$  coverage over  $\pm 1$  km. Long track.